

# Single Spark Numerical Modelling of Wire Electrical Discharge Machining for Solar Photovoltaic Applications

Aaditya S. Parasrampuria

*<sup>1</sup>Singapore International School, on National Highway No. 8, Post Mira Road, next to Thakur Mall, Dahisar East, Mumbai, Maharashtra -401104, India*

-----\*\*\*-----

**Abstract :** Most renewable energy resources are marred with low conversion efficiencies which leads to longer payback time. Existing commercial solar cells exhibit an efficiency of around 14-19%. It can be improved considerably with Wire Electrical Discharge Machining (Wire-EDM) for slicing Si ingots as it can produce thinner wafers. The induced thermal damage is one of the major limitations while using the Wire-EDM process for solar cell applications. This work presents a study on reducing the thermal damage associated with Wire-EDM. The radius of the spark between the wire and the Si work-piece is very small compared to the width of the cut, therefore, it is possible to model the Wire-EDM process by considering a two-dimensional axis-symmetric model. The model was created and simulated in ABAQUS™ for a single spark between the slicing wire and the Si ingot. It was observed that spark energy is the most influential process parameter and can be controlled with pulse-on time and current. The relationship between applied current, pulse-on time with thermal damage, and temperature of the work-piece was evaluated. A parametric study revealed that the thermal damage could be brought down by 37 % and 22 % with reduction in current and pulse-on time respectively. Solar energy is one of the most wide-spread and economic sources of renewable energy. Such work can lead to improved efficiencies of solar photovoltaic and hence aid in reducing emissions globally.

**Keywords:** Wire-EDM process, Si wafers, solar cell, finite element modelling, thermal damage

## 1. Introduction

Solar energy has gradually turned into a mainstream source of power from its alternative energy status a few years ago. This surge in installation and utilization is mostly due to the solar photovoltaic (PV), which accounts for a huge share in total solar energy installed capacity [1]. High utilization of any technology calls for research to increase its production and operational efficiency. Solar PV modules are made from arrays of solar cells. These cells are manufactured with a thin wafer of silicon (Si) with various coatings and components on it. Slicing Si wafers from ingots is one of the most energy-intensive processes of solar cell manufacturing. Even a small improvement in this process will scale up to substantial cost savings in the overall context.

Generally, wafer slicing is done using diamond or abrasive wire sawing process [2]. The constraint of these methods is the lower limit of thickness of the wafers obtained. The lower limit of wafer thickness with mechanical abrasive processes is approximately 180  $\mu\text{m}$  [3]. Thinner wafers enable better efficiency of the solar photovoltaic cells. Producing wafers using wire-Electrical Discharge Machining (wire-EDM) process can be one of the solutions to this constraint. In wire-EDM, material removal is done using electrical sparks generated between the work-piece and a moving wire immersed in a dielectric liquid. This electrical spark method enables localized material removal resulting in an overall reduction of thickness [4]. However, it comes with its own set of limitations. Each electrical discharge generates heat energy in a narrow area that locally melts and evaporates the work-piece. Some of the melted and evaporated material is then quenched and flushed away by a dielectric liquid and the remaining melt gets recast on the finished surface. During sparking between the work-piece and wire, rapid heating of the sample takes place. The specimen is immediately cooled off as well due to the flow of dielectric liquid around it. The quenching (cooling) rate is the same everywhere, which leads to production of residual stresses.

The damaged region and recast layer on the sliced surface are removed by post-processing methods like polishing and etching, leading to loss of valuable material and increasing the cost of post processing. These limitations of residual stresses and wastage of material can be overcome to an extent with optimizing process parameters. Many process variables affect the surface integrity such as pulse duration, peak current, and open gap voltage among others. Also, the slicing rate and surface finish can be improved with optimized parameters to achieve the enhanced overall efficiency of a solar cell. Experimental ways of improving the wire-EDM operation will require a significant number of experiments due to large number of process parameters. Numerical modelling of wire-EDM can help researchers to identify particular pain points with comparative ease and work towards resolving them.

Attempts at modelling the process started with DiBitonto et al. [5], where the researchers have obtained temperature profiles [6], heat-affected zone, and dimensions of the craters formed using computational methods. However, most of these studies were conducted for the EDM process with die-sinking, and not on the slicing method of material removal used in wire-EDM. Although comparative studies of different models such as the one by Yahya et al. [7] are genuinely informative and can be used as a base for many subsequent attempts at improving the process. An optimized set of universally accepted process parameters is still an area of concern and would require a considerable amount of input in terms of numerical modelling with as realistic settings as possible.

Another approach to optimize the parameters is through the Response Surface Methodology (RSM). RSM is a statistical method to explore the correlation between different variables of a process and determine the influence of various controlling factors. Generally, a 3k factorial design is used to evaluate k factors. Each at three levels (low, intermediate, and high). These are expressed as -1, 0, and 1 numerically. Three-level design is used to model the possible curvature in the response function and to handle the case of nominal factors at three levels. However, in order to be used in experiments, a three-level design can still be time-consuming as the total runs will come very high when the number of factors is more.

This work is an attempt to generate a robust set of process parameters for the optimized performance of Wire-EDM wafer slicing of silicon ingots to create wafers for solar cell applications. A two-dimensional asymmetric model was created in ABAQUS™ to assess the temperature profile and subsequent thermal damage. RSM is utilized to identify the optimum processing conditions for the least damage. Initially, the aim is to conduct a parametric study and identify crucial parameters. At the elementary level, modelling of the process can be seen as solving a heat diffusion equation at the interface of slicing wire and work-piece. Here the heat source would be the plasma generated in the spark during the process and considered as surface heat flux. The simulation results are then compared to experimental values in the literature to validate the model. Overall, such a study will benefit the solar energy industry and help humanity to tackle the menace of climate change in a slightly more efficient manner.

As a future prospect, the thermal damage can enable us to determine the fatigue life of the silicon wafer. Also, numerical optimization methods can be utilized along with experiments to maximize throughput of the process.

## 2. Results and Discussion

In the present section, the ABAQUS simulation results such as maximum surface temperature, thermal damage, and temperature variation with time are explained.

### 2.1. Temperature profile

These simulations have revealed the extent and intensity of heat diffusion for a single spark between the work-piece and wire. Figure 2 depicts temporal variation of the radial temperature distribution of work-piece around the centre of the spark. These results are corresponding to a current of 0.5 A, and on-time of the spark is 25  $\mu\text{s}$ , which is initiated at  $t = 0$ . The maximum temperature obtained of the work-piece is around 4000K, and as expected, the heat is confined to the vicinity of the centre of the spark at the end of the pulse at  $t_p = 0.25 \mu\text{s}$  as seen in figure 2(a). Furthermore, figure 2(b) shows the temperature distribution at  $t_p = 3 \mu\text{s}$  which is considered very late as compared to the duration of the pulse-on time of the spark. Although the temperatures have reduced to a great extent, the heat diffusion has increased. A similar trend is observed at  $t = 8.25 \mu\text{s}$  and 15  $\mu\text{s}$  seen in figure 2(c), and (d), the maximum temperature obtained has reduced, and heat diffusion in the work-piece has increased to a large extent.

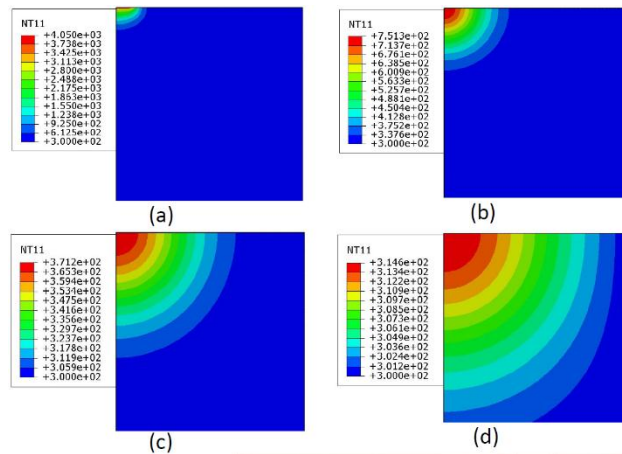


Figure 1 Temperature contour at different time step (a) 0.25  $\mu$ s (b) 3  $\mu$ s (c) 8.25  $\mu$ s (d) 15  $\mu$ s

Figure 3 shows the variation of maximum obtained temperature with a pulse-on time used for simulation. This relationship is depicted for three different values of current. It was noticed the value of maximum temperature increases with an increase in pulse-on time, which can directly be attributed to the enhanced amount of heat input as a result of the increased time of spark. It can be deduced that longer the spark remains on, higher will be the work-piece temperature. Another observation from this result is the change in highest temperature with the value of current. The heat input will increase with current, however, this increase varies with pulse-on time of the spark. At lower pulse-on-time (0.25  $\mu$ s), the highest temperature of the specimen is around 250K, whereas, at the higher pulse-on time (0.75  $\mu$ s), increase in highest obtained temperature is about 800K. This behaviour can be attributed to the relationship between current and heat generated. The amount of heat generated varies with the square of the current, and hence as the value of current increases, the difference in temperature will also increase. When the value of pulse-on-time reduces by 67 %, there is a 32 % reduction in maximum surface temperature. This change is more or less similar for all the current values.

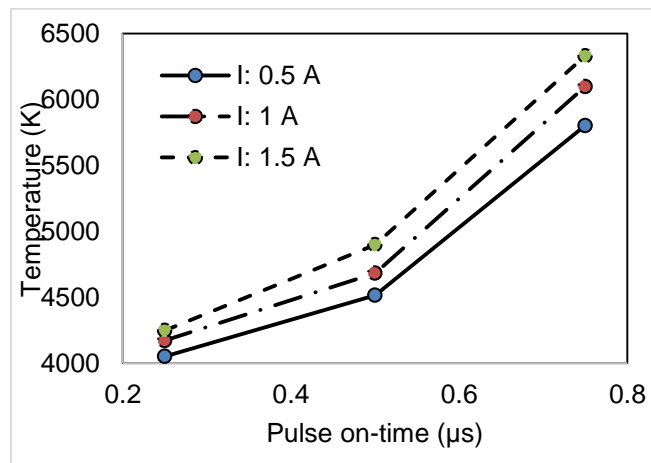


Figure 2 Variation in maximum temperature with pulse-on time at a different value of current

In Figure 4, the variation in temperature with the current at different values of pulse-on time is illustrated. From the figure, it can be observed that the temperature increases linearly with an increase in current. However, the rate of change is slightly different. At lower values of current, the surface temperature is higher in the case of high pulse-on time than the low pulse-on time. This is because with an increase in pulse-on time, pulse energy increases, resulting in more diffusion of heat in the material. Once the pulse-on time crosses the 0.5  $\mu$ s value, then the rate of increase in temperature escalate drastically. When the value of the current is reduced by 67 %, there is a 16 % reduction in the maximum surface temperature. From Fig. 3 and 4, it can be concluded that pulse-on time has more influence on surface temperature than the current value. This phenomenon is more or less common for all the pulse-on time.

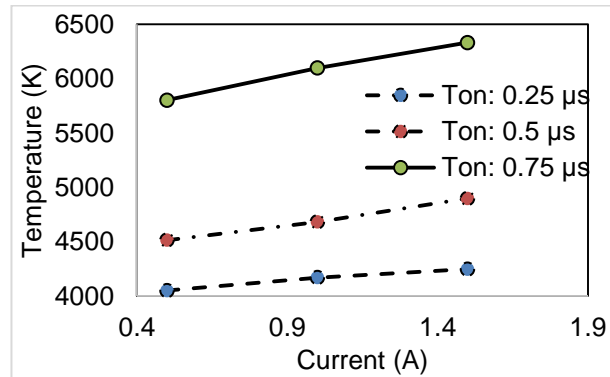


Figure 3 Variation in maximum temperature with a current at a different value of pulse-on time

## 2.2 Thermal Damage profile

In this section, thermal damage is evaluated from the temperature profile. Figure 5 shows the sample calculation of thermal damage in which the temperature along the depth is plotted at different time steps. The average boiling temperature of the Si is 3450K, and the recrystallization temperature is around 800K. It is assumed that material having a temperature above the boiling point is getting evaporated, and the region between recrystallization and boiling temperature is considered as thermal damage region. The horizontal line is drawn at 3450K and 800K [9], represented by a red line. When these red lines intersect temperature, curve draws the vertical lines from those particular points. These vertical lines intersect the x-axis, and the distance between the vertical line gives the value of the thermal damage.

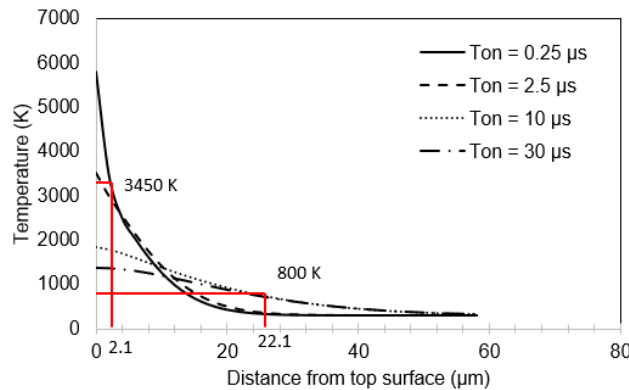


Figure 4 Variation in temperature along with the depth at different time step

It is assumed that material having a temperature between liquidus and boiling point is melted and re-solidified over the surface. The thermal damage variation with a pulse-on time at a different value of current is evaluated from the temperature profile is shown in Fig. 6. It can be observed that with an increase in pulse-on time, thermal damages increase continuously because, heat flux value increases with pulse-on time as a result of higher spark energy. Due to high spark energy, the maximum temperature achieved at the surface is also high. More heat can be diffused in the material, so microstructural changes occur at the depth resulting in higher thermal damage. The rate of change in thermal damage is similar at all values of current. At the intermediate value of pulse-on time, there is marginal variation in thermal damage with the current compared to extreme values. When the value of pulse-on-time reduces by 67 %, there is a 37 % reduction in the thermal damage value for all the value of current.

In Fig, 7, the thermal damage variation with the current at a different pulse-on time is shown. With an increase in current value, thermal damages decrease continuously for all value of pulse-on time. The decline in thermal damage is marginal for the 0.5  $\mu\text{s}$  value of pulse-on time, whereas for 0.25  $\mu\text{s}$  and 0.75  $\mu\text{s}$  case, there is a sharp reduction in thermal damage.

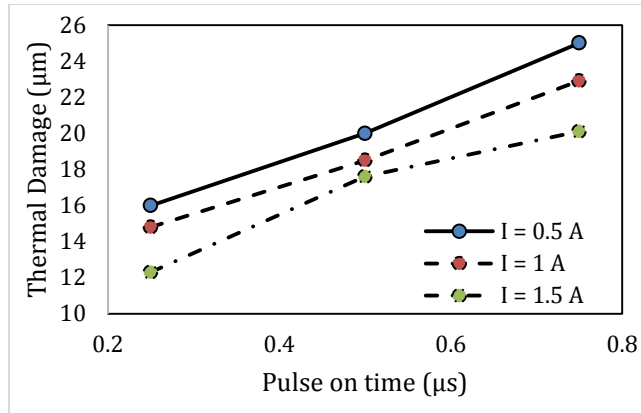


Figure 5 Variation in thermal damage with pulse-on time at different current

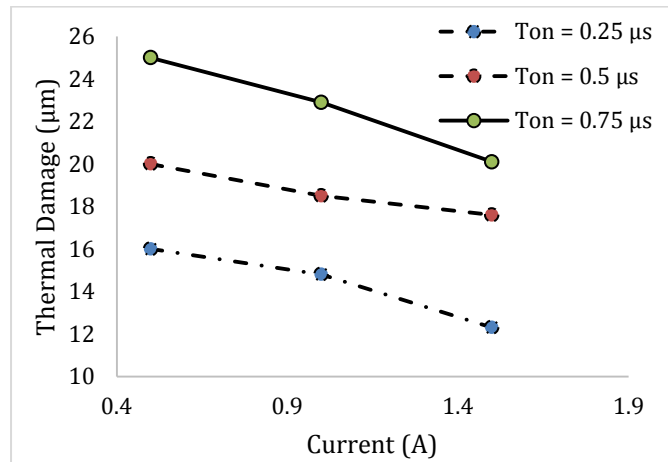


Figure 6 Variation in thermal damage with the current at a different value of pulse-on time

**Conclusion**

Simulations of the wire-EDM process for slicing Si wafers were performed. It was found that thermal damage in the work-piece is mainly affected by pulse energy, which in turn depends on the current and pulse-on time of the wire-EDM process. Higher the pulse energy, greater the amount of heat diffused in the material resulting in high values of thermal damage. It was also deduced that pulse-on time has more influence on thermal damage than the current. When the value of pulse-on time decreases by a 67 %, there is a 37 % reduction in thermal damage, whereas a 67 % reduction in current value leads to a 22 % reduction in thermal damage value.

**Method (Modelling Approach)**

In this work, a 2D axisymmetric transient model of the EDM process is developed to estimate the temperature profile for a single spark. The 2D axisymmetric assumption is justified as the heat diffusion length in a single pulse is typical of the order of a few micro-meters, which is much smaller than the thickness of the work-piece. Pulse-on time used in the present work is in the range of 0.25 - 0.75  $\mu\text{s}$ , which is comparable to the discharge time. Therefore, it is assumed that only a single spark occurs in one pulse.

Figure 1 shows the schematic diagram of the EDM model. The 2-D axisymmetric model is developed to predict thermal damage through temperature profile. As machining occurs, the discharge should occur randomly all over the work-piece surface close to the wire. The temperature effects are obtained from this discharge model. The plasma energy from discharge is dissipated heat into the work-piece, and the rest is lost into the dielectric. It is assumed that plasma is at a constant temperature. Other effects of radiation and wire vibration are ignored in the model.

Table 1 Process parameters

Voltage	Current	Pulse-on time
110	0.5	0.25
110	0.5	0.5
110	0.5	0.75
110	1	0.25
110	1	0.5
110	1	0.75
110	1.5	0.25
110	1.5	0.5
110	1.5	0.75

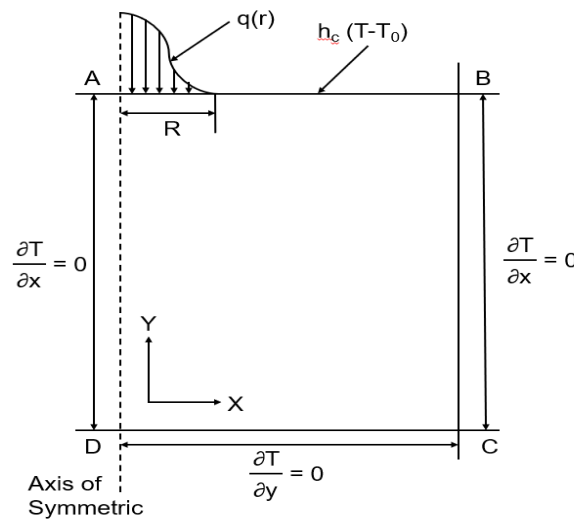


Figure 7 Modeling approach

The heating process can be modelled using the standard Fourier heat diffusion equation, which is given by:

$$\frac{\partial^2 T}{\partial x^2} + \frac{\partial^2 T}{\partial y^2} = \frac{\rho C}{k} \frac{\partial T}{\partial t} \quad (1)$$

Where  $k$  is the thermal conductivity of electrodes (W/m.K),  $T$  is the temperature (K),  $C$  is the specific heat capacity of solid material (J/kg.K),  $\rho$  is the density of electrode materials (kg/m<sup>3</sup>), and  $x$  and  $y$  are the coordinates axes. The above heat diffusion equation is solved by accounting for the plasma heat source term ( $Q(r)$ ). The areas where the dielectric is in contact with the work-piece are treated as a convective boundary, and all other surfaces are treated as adiabatic boundaries, as shown in Fig. 1. In mathematical terms, the applied boundary conditions are:

- $Q(r)$  on a top-left surface
- $h(T - T_0)$  on a top surface
- $\partial T / \partial t = 0$  on right and bottom surface

- Initial condition  $T = T_0$

Where  $T_0$  is the room temperature (K), and  $h_c$  is the convective heat transfer coefficient of the dielectric medium ( $W/m^2K$ ). The plasma heat source  $Q(r)$  is given by [12]:

$$Q(r) = \frac{4.45 \times 0.18 \times V \times I}{\pi \times R^2} \quad (2)$$

Where 0.18 is the fraction of heat input to the anode surface,  $V$  is the discharge voltage (V), and  $I$  is the discharge current (A), and  $R$  is the plasma channel radius, given by [REFERENCE]:

$$R = 2040 \times I^{0.43} \times T_{on}^{0.44} \quad (3)$$

The governing equations are solved using the finite element method in ABAQUS™. A 4-node linear heat transfer quadrilateral element (DC2D4) is selected. The materials properties used in the model are given in Table 2 [8].

Table 2 Properties of Si

Material Properties	Value
Density	2390 Kg/m <sup>3</sup>
Poisson Ratio	0.27
Latent Heat	13679656 J/Kg K
Young Modulus	150 GPa
Liquidus Temperature	1790 K
Solidus Temperature	1700 K
Conductivity	370 W/m k

## Acknowledgements

The author would like to express their gratitude towards 7on7 Academy, Mumbai, for providing regular guidance and inputs regarding various topics.

## References

1. Sukhatme, S.P. and Nayak, J.K., 2017. Solar energy. McGraw-Hill Education.
2. Hardin, C.W., Qu, J. and Shih, A.J., 2004. Fixed abrasive diamond wire saw slicing of single-crystal silicon carbide wafers. *Materials and manufacturing processes*, 19(2), pp.355-367.
3. Joshi, K., Ananya, A., Bhandarkar, U. and Joshi, S.S., 2017. Ultra thin silicon wafer slicing using wire-EDM for solar cell application. *Materials & design*, 124, pp.158-170.
4. Lauwers, B., Kruth, J.P., Liu, W., Eeraerts, W., Schacht, B. and Bleys, P., 2004. Investigation of material removal mechanisms in EDM of composite ceramic materials. *Journal of Materials Processing Technology*, 149(1-3), pp.347-352.
5. DiBitonto, D.D., Eubank, P.T., Patel, M.R. and Barrufet, M.A., 1989. Theoretical models of the electrical discharge machining process. I. A simple cathode erosion model. *Journal of applied physics*, 66(9), pp.4095-4103.
6. Patel, M.R., Barrufet, M.A., Eubank, P.T. and DiBitonto, D.D., 1989. Theoretical models of the electrical discharge machining process. II. The anode erosion model. *Journal of applied physics*, 66(9), pp.4104-4111.
7. Yahya, A., Trias, A., Erawan, MA, Nor Hisham, K., Khalil, K. and Rahim, M.A.A., 2012. Comparison studies of electrical discharge machining (EDM) process model for low gap current. In *Advanced Materials Research* (Vol. 433, pp. 650-654). Trans Tech Publications Ltd.
8. Jilani, ST and Pandey, P.C., 1982. Analysis and modelling of EDM parameters. *Precision Engineering*, 4(4), pp.215-221.
9. Harris, G.L. ed., 1995. Properties of silicon carbide (No. 13). Iet.

## Author

I, Aaditya Parasrampur, am currently in high school where I am pursuing the IBDP curriculum. Being really intrigued by all STEM subjects, I especially look forward to pursue Engineering at College. I look forward to further my knowledge in this field by either taking civil or materials engineering at college.